Characterization of the propagation channel for urban UAV applications

Marwan El Hajj, Gheorghe Zaharia, Ghais El Zein, Nathalie Banoun

Characterization of the propagation channel for urban UAV applications

Marwan El Hajj*, Gheorghe Zaharia†, Ghais El Zein†, Nathalie Banoun*
* Capgemini Engineering, France
Email: {marwan.el-hajj;nathalie.banoun}@capgemini.com

†Univ Rennes, INSA Rennes, CNRS, IETR, UMR 6164, F 35000, Rennes, France
Email: {gheorghe.zaharia;ghais.el-zein}@insa-rennes.fr

***Abstract*—To meet the large demand for online orders in the last years, especially after the COVID-pandemic, a new paradigm of parcel delivery is in progress deployment. It's the drone delivery. In this work, we provide a statistical propagation model for the Air-to-Ground (A2G) path loss between an Unmanned Aerial Vehicle (UAV) and a ground terminal. The model is based on urban microcell characteristics. The simulations were carried out using the NYUSIM simulator at two frequency bands: 2.4 GHz and 5.8 GHz. Moreover, two scenarios were considered for simulations: the line of sight (LOS) and the non-line of sight (NLOS). The path loss function of distance, the excessive path loss, the RMS delay spread, and coherence bandwidth were studied in this paper.**

***Index Terms*—Unmanned aerial vehicle, air-to-ground propagation channel, excessive path loss, delay spread, coherence bandwidth**

I. Introduction

Unmanned Aerial Vehicles (UAVs) known as drones, small planes, and balloons are increasingly in demand due to their important role in multiple fields and applications. Indeed, UAVs are a part of Autonomous Systems (AS) such as robots performing tasks without human involvement [1], [2]. UAVs provide reliable, environmentally friendly, easy, fast, and cost-effective solutions for various scenarios and applications.

Thanks to recent technological innovation, various applications of drones can be cited: on the one hand, drones can be deployed as aerial base stations (BS) for a fixed term, particularly in very dense areas such as during a soccer match to enhance coverage and capacity of beyond 5G wireless cellular networks. On the other hand, drones can be used as aerial user equipment (UE) connected to a ground user (mobile phone or platform). As UE, UAVs play an important role in the Internet of Things (IoT) scenario whose devices are not able to communicate over a long range. Examples include surveillance, package delivery, and traffic monitoring scenarios.

In recent years, drone parcel delivery and vehicle routing problem have become the research topic of several international companies like Amazon and DHL [3], [4]. The last-mile delivery is the final step in the logistic delivery supply chain. It's the most expensive "end node", their cost varies from 13% to 73% concerning the total distribution cost [5]. The use of unmanned aerial vehicles in the delivery process reduces noise, congestion in the urban area, and CO_2 emissions. Otherwise, drones have lower capacity and working time (low flight endurance) than fuel-powered vehicles. Drones can transport low-weight packages and reduce turnaround times, which also increases enabling more deliveries per day and reduces the transportation costs of the delivery process.

In the parcel delivery scenario, we consider that the drone is a UE connected to a ground user (truck). Establishing good communication between drone and truck requires an accurate air-to-ground channel model [6]–[8]. The A2G channel characteristics significantly differ from ground-to-ground or air-to-air channels. UAV-to-ground channels are more susceptible to blockage [1] and are dependent on altitude, elevation angle, shadowing effect, and type of propagation environment.

Many studies focus on the characterization and modeling of the A2G channel in recent years. We can categorize these studies into two types: *payload communications* are mostly application dependent and *control non-payload communications (CNPC)* for telemetric control of UAVs. Usually, the unlicensed bands (2.4 GHz and 5.8 GHz) are used for the CNPC. However, another frequency band (3.4 GHz) can be used for additional features such as transferring videos from the drone to the ground station [9]. In [10], [11] the authors provide the basic characteristics of the A2G channel with the limitations of the existing models. They conducted measurement campaigns also in a suburban/hilly environment and provided model results for propagation path loss, Rice's K-factor, delay spread, and fading in A2G communications. In [7], the authors provide modeling and simulation of rain attenuation, cloud attenuation, gaseous absorption attenuation, and Ricean fading for High Altitude Platform stations (HAPs). In [8] the authors introduce a propagation model for mobile communications from HAPs in different types of built-up areas as a function of the angle of elevation. Finding a generic channel model for A2G communications requires comprehensive simulations and measurements in various environments.

In this work, we provide a characterization of the air-to-ground propagation channel in an urban microcell environment. We consider two scenarios: the line of sight (LOS) and the non-line of sight (NLOS) scenario between a base station acting as a drone and a user at street level. We selected two frequency bands (2.4 GHz and 5.8 GHz) for the UAV applications.

The paper is organized as follows: Section II describes the NYUSIM simulator, the simulation scenario, and parameters. Section III presents the simulation results and analysis. Finally, Section IV sums up several conclusions.

II. NYUSIM Simulations

A. Overview Of NYUSIM

NYUSIM is an open-source channel simulation software, developed by NYU Wireless academic research center at New York University using MATLAB [12], [13]. The simulator is based on extensive propagation channel measurements conducted in various outdoor and indoor environments at millimeter-wave (mmWave) and sub-Terahertz (THz) waves. Examples of such environments include urban macrocell (UMa), urban microcell (UMi), rural macrocell (RMa), indoor factory (InF), and indoor office hotspot (InH) environments. NYUSIM can operate over a wide range of carrier frequencies starting from 500 MHz to 150 GHz and support wide RF bandwidth up to 800 MHz. NYUSIM generates the temporal and spatial channel impulse response (CIR) for the omnidirectional and directional channel model. Two running simulation modes are implemented in the simulator: the drop-based mode and the spatial consistency mode. The drop-based mode signifies a generation of random and independent channel simulations for fixed or range transmitter-receiver (Tx-Rx) separation distance. The spatial consistency mode provides a continuous and realistic evolution of the channel along a user terminal (UT) trajectory in a local area [13]. Moreover, NYUSIM provides as output the omnidirectional and directional channel models to accurately design and implement uniform linear and rectangular antenna arrays (ULA and URA) to exploit spatial diversity and/or beamforming gain in multiple-input multiple-output (MIMO) systems. In [14], further information is given on the Matlab code used in NYUSIM, applications, and channel models.

B. Simulation scenario

To ensure reliable and fast delivery, the drone will be used for parcel delivery in an urban environment. Due to the limited capacity in terms of resources, the drone will be aided by a truck on the ground considered as a mobile depot. The truck will not only be used for drone departure and landing, drone refueling, or battery charging but also to deliver heavy loads to customer locations. The truck will be in continuous communication with the drone for any unforeseen event occurring during delivery, for example in case of the falling package before arriving to the customer. Fig. 1 illustrates the virtual-city environment in a downlink communication from the UAV to the truck with Tx-Rx separation distances d_{min}, d_{max} of 10 m and 500 m respectively. α is the elevation angle between the horizon and the LOS truck-UAV. α is at max for d_{min} and minimum for d_{max}. As shown in Fig. 1 the air-to-ground channel is composed of two segments, the free space path loss (FSPL) segment and the urban segment. The FSPL segment is considered when the propagation passes over the tallest building in the geographical considered area. Otherwise, the urban segment corresponds to the case where wave propagation takes place between the ground and the tallest building.

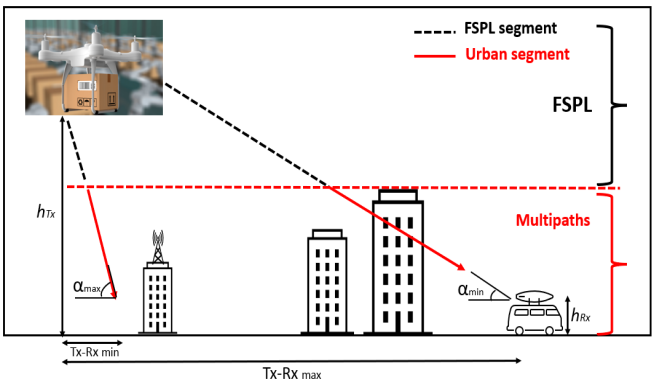

Figure 1: The virtual-city simulated.

C. Simulation parameters

Before launching the simulation, some parameters must be chosen from the graphical user interface (GUI). We start by choosing the drop-based mode simulation and then the channel parameters of the UMi environment like carrier frequency, RF bandwidth, LOS/NLOS scenario, lower and upper bound of Tx-Rx separation distance, transmitted power, heights of the transmitter and the receiver, and polarization. Environment parameters such as barometric pressure of 1013.25 mbar, and humidity of 50% are taken as default. Delivery of the package will take place on a day without rain, with a temperature of 20°C. There is no foliage taken into consideration in our simulations. Regarding the antennas, we consider a SISO scenario: an omnidirectional antenna, with an aperture of 45° at -3 dB beam-width (HPBW) in the elevation plane for both the transmit and the receive sides. Table I shows all parameters considered in the simulation to provide the received power and the path loss. The drone is considered as a transmitter and the truck as the receiver, but due to channel reciprocity, the roles can be reversed.

III. Simulation Results and analysis

A. Radio channel and path loss

To study the path loss variations between the UAV and the truck, we simulated 1000 randomly distributed receiver positions where the received power and then

Table I: Simulation parameters

Center frequency	2.4 GHz and 5.8 GHz
Simulation environment	UMi
Bandwidth	800 MHz
Scenario	LOS/NLOS
Number of receiver locations	1000
Distance range option	10 to 500 m
Transmitted power	0 dBm
Drone height	36.5 m
Truck height	1.5 m
Lower bound	10 m
Upper bound	500 m
Tx HPBW azimuth	360°
Rx HPBW azimuth	360°
Tx HPBW elevation	45°
Rx HPBW elevation	45°
Polarization	Co-polar

the path loss are calculated. The 1000 positions vary between d_{min} and d_{max} which will also vary the elevation angle, noted by α_{max} and α_{min}. The elevation angle, seen from a certain receiving point, is calculated by $\alpha = \tan^{-1}(\frac{h_{Tx}-h_{Rx}}{d_{T_x-R_x}})$. The $PL_{LOS/NLOS}$ path loss[dB] impairing a transmitted signal from the UAV to the truck in LOS or NLOS, can be written as:

$$PL_{LOS/NLOS}[dB] = P_{T_x}[dBm] - P_{R_x}[dBm] \quad (1)$$

where $P_{T_x}[dBm]$ is the UAV transmitted power and $P_{R_x}[dBm]$ is the power at the receiving point. Moreover, this air-to-ground path loss (in dB) again referred to as the air-to-ground path loss, can be expressed as the sum of the FSPL between the UAV and the truck on the ground, which we will refer to as FSPL, and excessive path loss η, in the urban environment in the form of shadowing and scattering as mentioned in [6].

NYUSIM yields a list of the 1000 receiver positions, including corresponding path loss, T-R separation distance, and LOS/NLOS received power. This data is then further processed, to obtain the excessive path loss component as defined in [6]:

$$\eta_{LOS/NLOS}[dB] = PL_{LOS/NLOS}[dB] - FSPL[dB] \quad (2)$$

where FSPL is the free space path loss for the 3D T-R separation distance, obtained from Friis transmission equation [15], given by:

$$FSPL[dB] = 32.44 + 20log_{10}(f[GHz]) + 20log_{10}(d[m]) \quad (3)$$

where $d = \frac{\Delta h}{\sin\alpha}$ is the distance between the UAV and the receiver in meters, $\Delta h = h_{UAV} - h_{Truck}$ in meters with α the elevation angle seen from a certain receiving point. f is the carrier frequency in GHz. The simulations are performed for two different frequencies: at 2.4 GHz and 5.8 GHz for two scenarios, in LOS and NLOS. These choices make it possible to cover a wide range of applications.

B. Path Loss model

Fig. 2 presents the omnidirectional, directional, and best-directional path loss model in LOS at 5.8 GHz. The Close-In (CI) free space path loss model used in NYUSIM is :

$$PL^{CI}(f,d)[dB] = FSPL(f,d_0) + 10n\log_{10}(\frac{d}{d_0}) + AT[dB] + X_\sigma^{CI} \quad (4)$$

where $d(m)$ is the 3D T-R separation distance ($d \geq d_0$), $d_0 = 1m$ denotes the free space reference distance in meters, n is the path loss exponent (PLE), f the frequency in GHz. AT[dB] is the attenuation term induced by the atmosphere. AT is defined as AT[dB] $= \alpha[dB/m]\times d[m]$, where α is the attenuation factor in dB/m for the frequency range of 1 GHz to 100 GHz, which includes the collective attenuation effects of dry air (including oxygen), water vapor, rain, and haze, $d[m]$ is the 3D T-R separation distance as in (4). At lower frequencies (2.4 GHz and 5.8 GHz), AT[dB] is considered negligible. X_σ^{CI} is the zero-mean gaussian random variable with a standard deviation σ in dB.

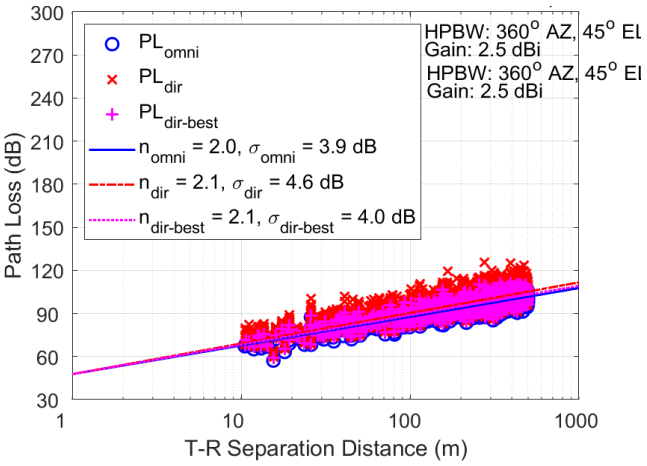

Figure 2: Omnidirectional, directional and best-directional path loss in LOS at 5.8 GHz provided by NYUSIM.

In the LOS scenario, the path loss exponent n is equal to 2 which corresponds to the free space case, and increases slightly to 2.1 for the directional case, as mentioned in Table II. The standard deviation σ in the omnidirectional case is equal to 3.9 dB while in

Table II: Path loss model parameters for LOS and NLOS scenarios at 5.8 GHz in UMi environment.

Frequency	5.8 GHz	
Scenario	LOS	NLOS
n_{omni}	2.0	3.2
n_{dir}	2.1	3.3
$n_{dir-best}$	2.1	3.2
σ_{omni} (dB)	3.9	6.8
σ_{dir} (dB)	4.6	6.9
$\sigma_{dir-best}$ (dB)	4.0	6.8

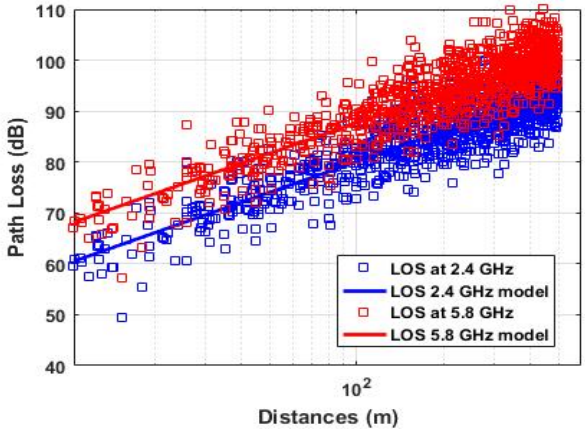

Figure 3: Omnidirectional path loss in LOS scenario at 2.4 GHz and 5.8 GHz in UMi environment.

the directional case σ increases by 0.7 dB concerning the omnidirectional case. The path loss model has more accuracy using an omnidirectional antenna at lower frequencies in urban environments. Figure 3 presents the omnidirectional LOS path loss for 2.4 GHz and 5.8 GHz. A difference of around 7 dB is noticed between the two models. Figure 4 presents the omnidirectional NLOS path loss for 2.4 GHz and 5.8 GHz. The losses increase in the NLOS scenario. It's around 12 dB and 13 dB concerning the LOS scenario at 2.4 GHz and 5.8 dB respectively.

In the NLOS scenario, the path loss increases, and n is around 3.2, which is normal behavior since we have different propagation phenomena like diffractions and reflections in the urban environment. The std is around 6.8 dB, which corresponds to lower precision than in the LOS scenario.

C. Probability distribution function

Fig. 5 illustrates the probability density function (PDF) histogram of the data set in the function of the excessive path loss η for LOS and NLOS scenarios. To model these two propagation groups, we propose the use of Gaussian

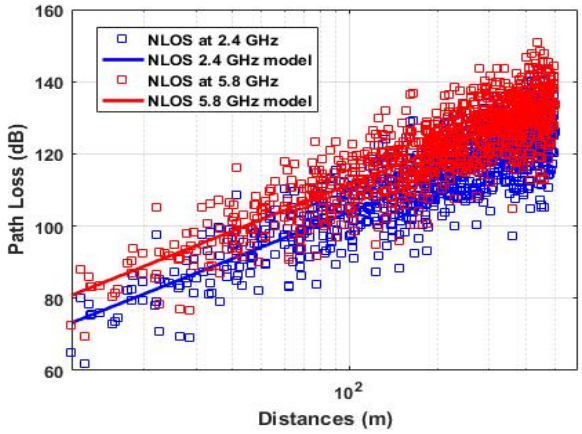

Figure 4: Omnidirectional path loss in NLOS scenario at 2.4 GHz and 5.8 GHz in UMi environment.

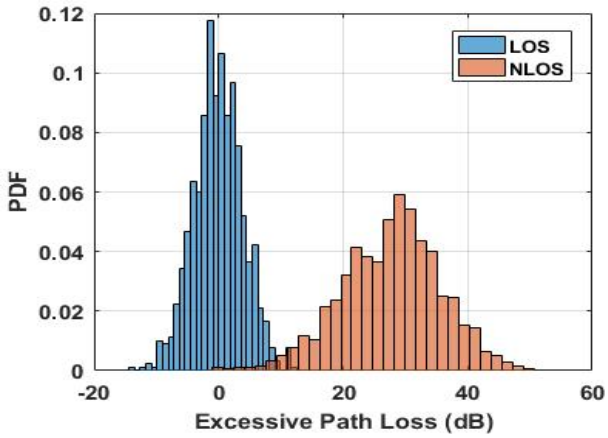

Figure 5: Excessive path loss samples histogram, obtained at 5.8 GHz for UMi environment in LOS and NLOS scenario.

distribution model expressed as the following equation:

$$f(\eta|\xi) = \mathcal{N}(\mu_\xi, \sigma_\xi^2) \tag{5}$$

where $\mathcal{N}$ is the normal distribution of a mean μ_ξ and a standard deviation σ_ξ. ξ represents the LOS or NLOS scenario. For each scenario, we study the statistical behavior by deducing the mean value and the standard deviation as represented in Table III.

Table III: RF model parameters for LOS and NLOS scenario at 5.8 GHz.

Frequency	5.8 GHz	
Scenario	LOS	NLOS
μ (dB)	-0.0271	27.7050
σ (dB)	3.9274	8.0187

Globally, the LOS and NLOS scenarios at 2.4 GHz

and 5.8 GHz have similar behavior. We note the same values of $\mu_{LOS/NLOS}$ and $\sigma_{LOS/NLOS}$ which may be due to the way to generate the data samples using predefined parameters-models taken by the NYUSIM simulator. In [6], the authors found a mean of excessive path loss for the urban environment in the LOS scenario of 1.0 dB and 1.2 dB at 2.4 GHz and 5.8 GHz respectively. Otherwise, in the NLOS scenario, the authors found a mean of 20 dB and 23 dB at 2 GHz and 5.8 GHz respectively. Compared to [6] no significant differences can be noticed for the LOS scenario, we note around 1 dB difference for μ_{LOS} and between 5 dB to 7 dB for μ_{NLOS}.

D. Excessive path loss in terms of elevation angles

Fig. 6 shows the excessive path loss for the two clusters of data-set samples, the LOS and NLOS, in terms of elevation angles at 5.8 GHz. NYUSIM provides many more received points for low elevation angles (high Tx-Rx distance) than higher ones. For this reason, we observe dense data points between 4^o and 20^o. We noticed from Fig. 6 that the samples tend to have a constant mean value by deducing the mean values in each scenario. The distribution of the excessive path loss samples around the means is more dispersive at lower elevation angles.

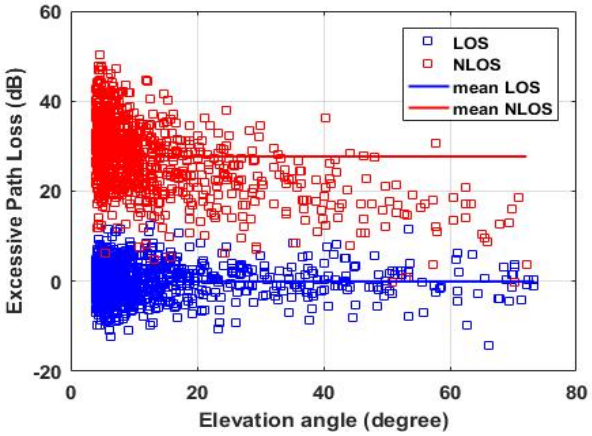

Figure 6: Excessive path loss in terms of elevation angle, obtained at 5.8 GHz for UMi environment in LOS and NLOS scenario.

E. RMS delay spread and coherence bandwidth

NYUSIM provides also the RMS delay spread τ_{RMS} of each Tx-Rx position for LOS and NLOS scenario. τ_{RMS} is an important parameter for any radio channel because it imposes a limitation to the symbol rate transmission to avoid intersymbol interference (ISI). Fig. 7 and Fig. 8 present the probability density function (PDF) and the cumulative distribution function (CDF) of the RMS delay spread at 5.8 GHz in LOS and NLOS scenario. The results show that the RMS delay spread remains globally below 30 ns in LOS versus 70 ns in NLOS.

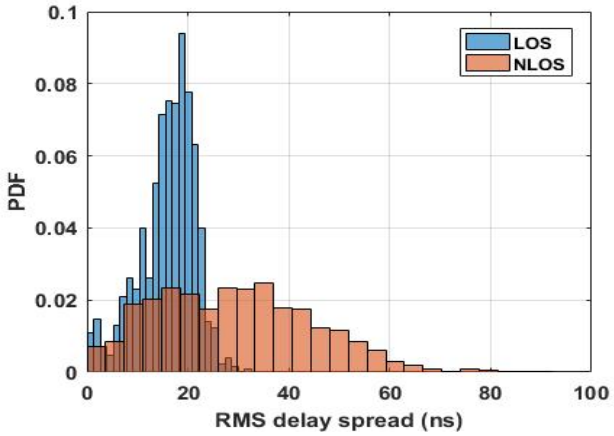

Figure 7: PDF of the RMS delay spread at 5.8 GHz for UMi environment in LOS and NLOS scenario.

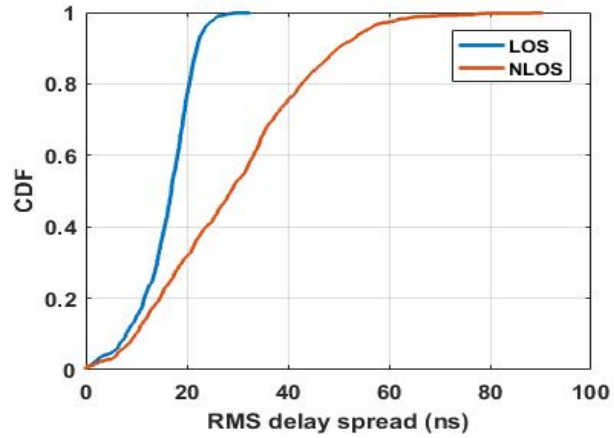

Figure 8: CDF of the RMS delay spread at 5.8 GHz for UMi environment in LOS and NLOS scenario.

In the same way, the coherence bandwidth Bc_{90} is a frequency characterization parameter of the channel. It corresponds to the frequency range over which the channel alters transmitted frequency components with approximately equal gain and linear phase. The channel can be considered flat in such conditions. Mathematically, the coherence bandwidth is defined as the frequency range over which the autocorrelation of the Fourier transform of the power delay profile (PDP) is greater than a threshold γ. However, based on the value of the RMS delay spread, we can roughly calculate Bc_{90}, the coherence bandwidth for $\gamma = 90$ % [16] at each receiver point using approximation (6).

$$Bc_{90} \approx \frac{1}{50\tau_{RMS}} \tag{6}$$

Fig. 9 presents the CDF of the coherence bandwidth at 5.8 GHz in LOS and NLOS scenarios, respectively. We can notice that the coherence bandwidth in the LOS scenario is 2.3 times greater than in the NLOS scenario.

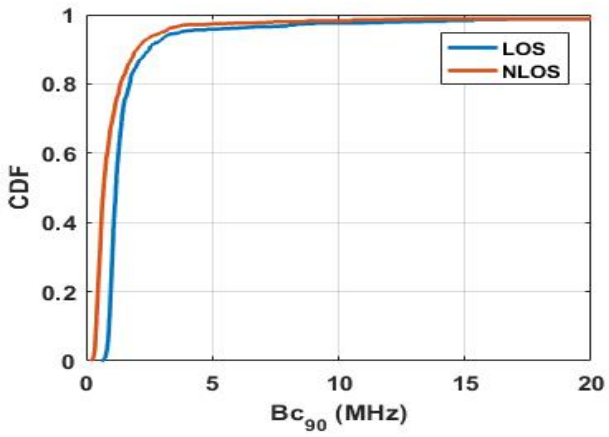

Figure 9: CDF of the coherence bandwidth Bc_{90} at 5.8 GHz for UMi environment in LOS and NLOS scenario.

IV. Conclusion

In this paper, we provide modeling of the air-to-ground propagation channel in the UMi environment. Two scenarios were considered: the LOS and NLOS. The targeted UAV application concerns radio links between a drone and a truck at street level. Two frequency bands were studied (2.4 and 5.8 GHz). The simulations carried out using the NYUSIM tool made it possible to model the propagation channel in LOS and NLOS, in the 2.4 GHz and 5.8 GHz bands. NYUSIM uses the CI free space path loss model. Analysis of the results in the 5.8 GHz band focused first on path loss as a function of Tx-Rx distance and elevation angle. Then, the analysis focused on the RMS delay spread and the coherence bandwidth of the propagation channel. Additional studies will be necessary to arrive at the finest possible modeling of this type of transmission.

Acknowledgement

This work was supported by Capgemini Engineering-France, under the project "ubiquitouS Platform for unmanned Aerial SystEms (SPASE)" in collaboration with INSA de Rennes.

References

[1] M. Mozaffari, W. Saad, M. Bennis, Y.-H. Nam, and M. Debbah, "A tutorial on uavs for wireless networks: Applications, challenges, and open problems," *IEEE communications surveys & tutorials*, vol. 21, no. 3, pp. 2334–2360, 2019.

[2] F. AlMahamid and K. Grolinger, "Autonomous unmanned aerial vehicle navigation using reinforcement learning: A systematic review," *Engineering Applications of Artificial Intelligence*, vol. 115, p. 105321, 2022.

[3] L. D. P. Pugliese, F. Guerriero, and G. Macrina, "Using drones for parcels delivery process," *Procedia Manufacturing*, vol. 42, pp. 488–497, 2020.

[4] W. Yoo, E. Yu, and J. Jung, "Drone delivery: Factors affecting the public's attitude and intention to adopt," *Telematics and Informatics*, vol. 35, no. 6, pp. 1687–1700, 2018.

[5] R. Gevaers, E. Van de Voorde, T. Vanelslander *et al.*, "Characteristics of innovations in last-mile logistics-using best practices, case studies and making the link with green and sustainable logistics," *Association for European Transport and contributors*, vol. 1, p. 21, 2009.

[6] A. Al-Hourani, S. Kandeepan, and A. Jamalipour, "Modeling air-to-ground path loss for low altitude platforms in urban environments," in *2014 IEEE global communications conference*. IEEE, 2014, pp. 2898–2904.

[7] Y. Zheng, Y. Wang, and F. Meng, "Modeling and simulation of pathloss and fading for air-ground link of haps within a network simulator," in *2013 International Conference on Cyber-Enabled Distributed Computing and Knowledge Discovery*. IEEE, 2013, pp. 421–426.

[8] J. Holis and P. Pechac, "Elevation dependent shadowing model for mobile communications via high altitude platforms in built-up areas," *IEEE Transactions on Antennas and Propagation*, vol. 56, no. 4, pp. 1078–1084, 2008.

[9] W. Khawaja, I. Guvenc, D. W. Matolak, U.-C. Fiebig, and N. Schneckenburger, "A survey of air-to-ground propagation channel modeling for unmanned aerial vehicles," *IEEE Communications Surveys & Tutorials*, vol. 21, no. 3, pp. 2361–2391, 2019.

[10] D. W. Matolak, "Air-ground channels & models: Comprehensive review and considerations for unmanned aircraft systems," in *2012 IEEE aerospace conference*. IEEE, 2012, pp. 1–17.

[11] D. W. Matolak and R. Sun, "Air–ground channel characterization for unmanned aircraft systems—part i: Methods, measurements, and models for over-water settings," *IEEE Transactions on Vehicular Technology*, vol. 66, no. 1, pp. 26–44, 2016.

[12] S. Sun, G. R. MacCartney, and T. S. Rappaport, "A novel millimeter-wave channel simulator and applications for 5g wireless communications," in *2017 IEEE international conference on communications (ICC)*. IEEE, 2017, pp. 1–7.

[13] S. Ju, O. Kanhere, Y. Xing, and T. S. Rappaport, "A millimeter-wave channel simulator nyusim with spatial consistency and human blockage," in *2019 IEEE global communications conference (GLOBECOM)*. IEEE, 2019, pp. 1–6.

[14] N. Y. University. (2023) NYUSIM. [Online]. Available: https://wireless.engineering.nyu.edu/nyusim-5g-and-6g/

[15] H. T. Friis, "A note on a simple transmission formula," *Proceedings of the IRE*, vol. 34, no. 5, pp. 254–256, 1946.

[16] T. S. Rappaport, "Wireless communications–principles and practice, (the book end)," *Microwave Journal*, vol. 45, no. 12, pp. 128–129, 2002.